Research Article

For reprint orders, please contact: reprints@futuremedicine.com

Nanomedicine

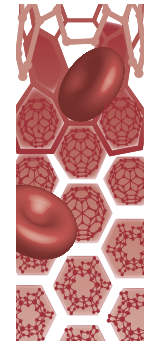

Rationalizing the use of functionalized poly-lactic-co-glycolic acid nanoparticles for dendritic cell-based targeted anticancer therapy

Background: Delivery of PLGA (poly [D,L-lactide-co-glycolide])-based biodegradable nanoparticles (NPs) to antigen presenting cells, particularly dendritic cells, has potential for cancer immunotherapy. **Materials & methods:** Using a PLGA NP vaccine construct CpG-NP-Tag (CpG-ODN-coated tumor antigen [Tag] encapsulating NP) prepared using solvent evaporation technique we tested the efficacy of *ex vivo* and *in vivo* use of this construct as a feasible platform for immune-based therapy. **Results:** CpG-NP-Tag NPs were avidly endocytosed and localized in the endosomal compartment of bone marrow-derived dendritic cells. Bone marrow-derived dendritic cells exposed to CpG-NP-Tag NPs exhibited an increased maturation (higher CD80/86 expression) and activation status (enhanced IL-12 secretion levels). *In vivo* results demonstrated attenuation of tumor growth and angiogenesis as well as induction of potent cytotoxic T-lymphocyte responses. **Conclusion:** Collectively, results validate dendritic cells stimulatory response to CpG-NP-Tag NPs *(ex vivo)* and CpG-NP-Tag NPs' tumor inhibitory potential *(in vivo)* for therapeutic applications, respectively.

First draft submitted: 14 August 2015; **Accepted for publication:** 16 December 2015; **Published online:** 19 February 2016

Keywords: breast cancer • cancer vaccines • DCs • dendritic cells • immunotherapy • nanoparticle • NP

Rutika A Kokate[1,2], Pankaj Chaudhary[1,2], Xiangle Sun[3], Sanjay I Thamake[1,2,4], Sayantan Maji[1,2], Rahul Chib[3], Jamboor K Vishwanatha[1,2] & Harlan P Jones*[,1,2]

[1]Department of Molecular & Medical Genetics, University of North Texas Health Science Center (UNTHSC), 3500 Camp Bowie Boulevard, Fort Worth, TX 76107, USA

[2]Institute of Cancer Research, University of North Texas Health Science Center (UNTHSC), Fort Worth, TX 76107, USA

[3]Department of Cell Biology & Immunology, University of North Texas Health Science Center (UNTHSC), Fort Worth, TX 76107, USA

[4]RadioMedix Inc., 9701 Richmond Avenue, Suite 222, Houston, TX 77042, USA

*Author for correspondence:
Tel.: +1 817 735 2448/0494
Harlan.Jones@unthsc.edu

Delivery vehicles for vaccines are of prime interest in the success of immune-based cancer therapies. Nanocarrier systems for the delivery of anticancer therapeutics have prompted special interests for the field of immunotherapy. In addition to loading chemotherapeutic drug candidates, the ability to encapsulate tumor-associated antigens (Ags) or peptide conjugates as immune stimulants are currently being pursued as primary cargo for nanocarrier systems [1]. The use of nanoparticles (NPs) is thought to increase the antigenic properties of encapsulated soluble Ags by increasing uptake by antigen presenting cells (APCs), particularly dendritic cells (DCs) [2,3]. Also, the large surface to volume ratio provided by NPs allows efficient surface functionalization which could be useful for cellular targeting purposes or secondary cargo loading. Furthermore, because tumor-associated Ags are weakly immunonogenic and result in weak vaccines resulting in poor tumor-specific immunogenicity, NPs could provide an additive immunogenic effect coupled with immune stimulants [4]. Thus fabrication on NPs can be customized to yield desired optimal properties, making codelivery of multiple agents possible [3].

Poly (D, L-lactide-co-glycolide) (PLGA)-based NPs have been extensively studied for developing Ag-based vaccines with controlled release properties. Biodegradable PLGA NPs have been designed to encapsulate both Ag and adjuvant inside the NP or on its surface [5]. The main advantage of using PLGA NPs from a vaccine perspective is that they serve as a safe, nontoxic mode of codelivery of Ag and adjuvant for a sustained period of

Future Medicine part of fsg

time [6–8]. Previous studies conducted and published recently by our group demonstrated that PLGA-based CpG-ODN-coated tumor antigen (Tag) encapsulating (CpG-NP-Tag) NPs were able to inhibit cancer cell, growth, proliferation and promote apoptotic cancer cell death *in vivo* associated with an increase in both $CD4^+$ and $CD8^+$ T-cell infiltration in tumor tissue [9]. However, further investigation is warranted linking NPs function as an immune-mediated mechanism.

The majority of literature claims that DCs, the 'professional APC' of the immune system, are the prominent initiators of Ag-specific immune responses and therefore are the key components of cancer vaccines [2]. Vaccination models involving DCs have been developed owing to their unique properties [10,11]. Induction of DC-based immune responses requires Ag uptake by DCs, its processing of said Ag and activation that produces a potent tumor-specific cytotoxic T-cell effector response against the tumor as well as the manifestation of immunological memory for the purpose of controlling tumor relapse [12–14]. Presumably, *ex vivo* pulsing of DCs (derived from patient) with Tag along with immune stimulants (such as GM-CSF or TLR agonists that induce DC maturation) followed by injecting cells back into patient is feasible for promoting antitumor immunity. Preliminary studies using *ex vivo* pulsed DCs have shown positive outcomes in some cancer patients but clinical trials in general show poor efficacy [15]. The current study sought to improve this experimental approach by testing an *ex vivo* system using bone marrow-derived dendritic cells (BMDCs) to determine the capacity of 'bacteriomimetic' surface-bound CpG-NP-Tag NPs to improve DC function and thus serve as an optimal candidate for *ex vivo* and possibly *in vivo* DC-based vaccine. In this article, we report mechanistic *ex vivo* studies using BMDCs to determine the ability of NP vaccine constructs to distinctively interact with DCs as potential for their use in particulate vaccine responses [2,10,15]. We also report the efficacy of this formulation to enhance CTL responses and impart antitumor immune responses *in vivo* in a syngeneic prophylactic 4T1 murine breast cancer BALB/c model. The results support the capacity of 'bacteriomimetic' CpG-NP-Tag NPs to improve DC function and thus serve as optimal candidates for *ex vivo* and possibly *in vivo* DC-based vaccines as therapies in the treatment of cancer.

Materials & methods

Materials

PLGA 50:50; inherent viscosity 1.13 dl/g; mw 50,000 was purchased from Lakeshore Biomaterials (AL, USA). Polyvinyl alcohol (mw 30,000–70,000; alcoholysis degree 88 ~ 99.9 (mol/mol)%) was purchased from Sigma-Aldrich (MO, USA). BS3 was purchased from Thermo Fisher Scientific (IL, USA). CpG-ODN 1826 (Class B CpG Oligonucleotide-Murine TLR9 ligand) was obtained from InvivoGen (CA, USA). RPMI 1640 media, Penicillin-Streptomycin (Pen-Strep), fetal bovine serum (FBS) were obtained from Invitrogen (CA, USA). Antimouse IFN-γ Alexa fluor 488, CD31 (platelet endothelial cell adhesion molecule) eFluor® 650NC, CD80 (B7–1) FITC, CD86 (B7–2) APC and CD107α Alexa fluor 488 purchased from ebioscience, Inc. (CA, USA).

Cell line

4T1 murine mammary carcinoma cell line was purchased from American Type Culture Collection (VA, USA) and was grown (passage 4) until 70% confluent in RPMI media supplemented with 10% FBS and 1% Pen-Strep.

Membrane lysate preparation

Membrane fraction of 4T1 cells was prepared using hypotonic buffer and dounce homogenizer followed by centrifugation at 5000 x *g* at 4°C for 15 min to pellet cell debris. Supernatant was collected and further centrifuged at 100,000 x *g* for 1 h at 4°C using N55 rotor to obtain the membrane lysate pellet. Final membrane fraction was washed with PBS and resuspended in 100–150 µl of RIPA buffer. Pierce™ bicinchonic acid protein assay kit (Thermo Scientific, IL, USA) was used to estimate the protein concentration.

Mice

Adult female BALB/c AnNHsd mice (5–6 weeks) were obtained from Harlan Laboratories, Inc. (IN, USA) and used for all studies. Mice were maintained at UNTHSC animal facility and allowed to acclimatize for a week prior to experimentation to avoid shipping stress. Mice were kept under optimal temperature and humidity conditions and provided with proper care under Institutional Animal Care and Use Committee guidelines. All procedures for the studies were in accordance with the Institutional Animal Care and Use Committee guidelines at UNTHSC.

Formulation of CpG-NP-Tag NPs

CpG-NP-Tag NPs were prepared using water-in-oil-in-water (w/o/w) double emulsion method employing solvent evaporation technique reported in our previous studies [9]. Briefly, primary emulsion (w/o) was prepared by vortexing a 200 µl of Tag solution (1 µg/µl) with 1 ml of organic phase (PLGA [70 mg] in ethylacetate [1 ml]). The primary emulsion (w/o) was added to 3 ml aqueous (w) phase (BS3 [0.5 mg/ml] in 1.1% polyvinyl alcohol). The mixture was sonicated on ice

using an ultrasonic processor UP200H system (Hielscher Ultrasonics Gmb, Germany) for 1–2 min to form activated NPs. After washing with 0.01% sucrose solution three-times these NPs were freeze dried and lyophilized (under 200 µm vacuum) on ATR FD 3.0 system and stored at -20°C until further use. For optimal conjugation of CpG, CpG ligand (1:200 w/w ratio) and resuspended NPs were incubated on an orbital shaker for 1–2 h at room temperature. After removal of excess ligand with PBS washes, CpG-coated Tag containing 'bacteriomimetic' NPs (CpG-NP-Tag) were obtained (Figure 1). CpG-NP-Tag NPs were characterized and subsequently used for *ex vivo* and *in vivo* studies.

Characterization of NPs

Particle size, polydispersity index, zeta potential & encapsulation efficiency

Particle size, polydispersity index (PDI) and zeta potential were measured using Zetasizer (Malvern Instruments Ltd.). A known quantity of NPs (0.25–0.5 mg) was resuspended in 1 m distilled water and further diluted 10-times before measuring particle size and zeta potential. Tag encapsulation efficiency was confirmed based on the amount of Tag (protein) extracted after degrading a fixed amount of NPs. 5 mg of NPs were degraded using 500 µl Acetonitrile (Sigma-Aldrich, MO, USA) by incubating at 37°C on a shaker (6–8 h). Samples were further centrifuged at 11,000 x *g* at 4°C for 10 min and the supernatants were tested for their protein content using bicinchonic acid protein assay kit (Thermo Scientific, IL, USA) as per manufacturer's instructions [16]. Encapsulation efficiency was calculated as follows: amount of protein encapsulated/amount of protein used in encapsulation × 100%.

Ligand binding efficiency

For evaluating CpG ligand binding efficiency, 0.5 mg of NPs were resuspended in distilled water and incubated with 14 µg of CpG-FITC for 60–90 min followed centrifugation and washing at 11,000 x *g* for 15 min to remove excess CpG ligand. Flow cytometry was conducted using a Beckman Coulter Cytomics FC

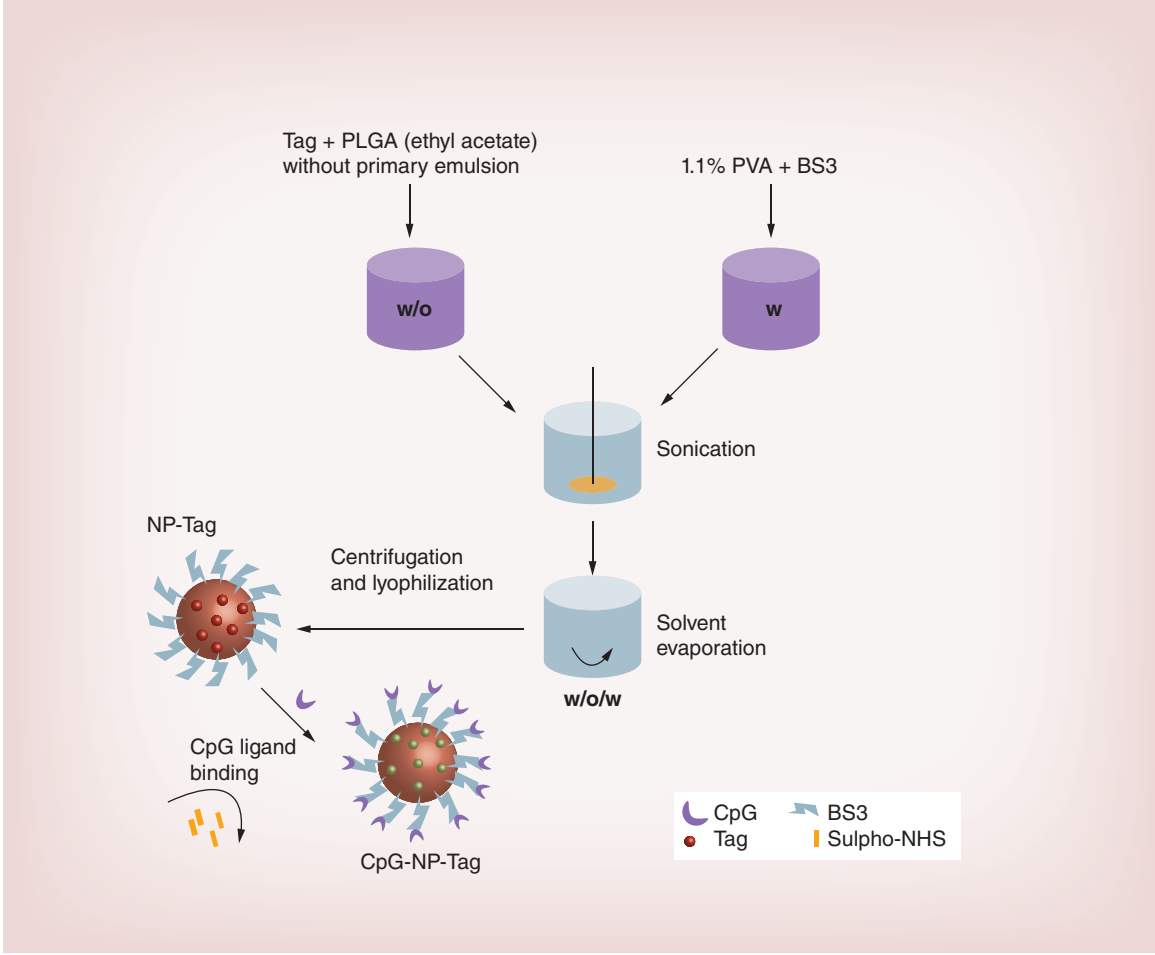

Figure 1. Formulation of nanoparticles. Schematic of the steps involved in the formulation of CpG surface-functionalized Tag-encapsulated NP (CpG-NP-Tag) and components of the NP.
NP: Nanoparticle; PLGA: Poly(lactic-co-glycolic acid); PVA: Poly(vinyl alcohol); Tag: Tumor antigen.

Table 1. Physicochemical characterization of nanoparticles.

Serial number	NP-construct	Particle size (nm ± SD)	Zeta potential (mV ± SD)	PDI	Encapsulation efficiency (%)	Encapsulation efficiency (µg/mg NP)
1	CpG-NP-Blank	230.6 ± 0.78	-1.14 ± 0.56	0.134	–	–
2	NP-Tag	227.3 ± 0.07	-0.51 ± 0.59	0.166	38.9 ± 5.7	4.2
3	CpG-NP-Tag	229.2 ± 0.71	-1.18 ± 0.39	0.13	38.9 ± 5.7	4.2

NP: Nanoparticle; PDI: Polydispersity index; SD: Standard deviation.

500 Flow Cytometer from core facility to determine the binding efficiency.

Scanning electron microscopy

SEM images were taken using Sigma VP Field Emission Scanning Electron Microscope manufactured by Carl Zeiss Microscopy Ltd. NP samples were coated with a Cressington108 Sputter Coater for 30 s. Target used for coating was an Au-Pd target.

Generation of bone marrow-derived dendritic cells

Briefly, mice were sacrificed with anesthesia followed by cervical dislocation, and rare legs were excised with two intact bones (femur-upper bone and tibia-lower bone). Every muscle and flesh was cleaned and the bones were placed in 70% ethanol in a petridish for 10 min. Bones were transferred to wash media (RPMI supplemented with 1% FBS and 1% Pen-Strep). One end of tibia (lower part) was cut and bone marrow cells were flushed out in an 50 ml conical tube using 27G needle and 10 ml syringe. Cells were centrifuged at 200 x *g* for 10 min and incubated with 10 ml ACK (ammonium–chloride–potassium) lysis buffer for 10 min to remove the red blood cells. Cells were centrifuged (300 x *g*) and resuspended in 1 ml culture media (RPMI media supplemented with 10% FBS, 1% Pen-Strep, 10 ng/ml GM-CSF and 10 ng/ml IL-4) and passed through mesh boat (to remove any debris) into a 60 mm culture plate containing 14 ml of culture media. On day 7 of the culture, BMDCs were transferred to either 6-well/12/24/96-well plates for different experiments [17]. Purity of BMDC population (50–55%) was evaluated using CD11c marker via flow cytometry for each set of experiment (data not shown).

BMDC NP uptake & intracellular localization

To evaluate uptake of the NPs flow cytometry was conducted using nile red stained NPs. BMDCs (~5 × 10^4) were plated in 6-well plates on day 6, and pulsed on day 7 with the respective groups of NPs (1–2 mg) for 1 h and processed for flow cytometric analysis. Briefly, cells were washed twice post NP incubation and trypsinized using 0.25% trypsin (Hyclone Laboratories, UT, USA). Cells were washed with staining buffer (one-times PBS and 1% FBS) and centrifuged for 10 min at 200 × *g*. Cells were fixed using 4% paraformaldehyde in dark for 20 min and analyzed the next day for NP uptake. Flow cytometry was conducted using a Beckman Coulter Cytomics FC 500 Flow Cytometer from core facility. For the purpose of intracellular (endosomal) localization, immunocytochemistry was conducted. Briefly, BMDCs were grown on cover slips in a 6-well plate and pulsed with a fixed quantity (1–2 mg) of nile red stained NPs for 1 h. Cells were washed twice with PBS and were incubated with an early endosome marker, EEA1 (primary) antibody overnight. Cells were washed thrice with PBS and incubated with secondary antibody conjugated to alexa fluor 488 for 1 h. Cells were fixed with 4% paraformaldehyde and mounted in a medium containing 1.5 µg/ml DAPI and confocal microscopy was used to study intracellular endosomal localization. Confocal microscopy was conducted utilizing LSM 510 META (Carl Zeiss).

BMDC maturation & activation

To evaluate the effect of NP immunization on APCs, BMDCs were derived from BALB/c mice as described above in 'Generation of bone marrow-derived dendritic cells' in 'Materials & methods'. At day 7 of the culture, BMDCs were pulsed with a fixed amount (1–2 mg) of different groups of NPs for 48 h. At day 9, BMDCs were processed for flow cytometry to determine the expression of maturation markers, CD80/86. Briefly, cells were washed twice post NP incubation and trypsinized using 0.25% trypsin (Hyclone Laboratoroes, Utah). Cells were washed with staining buffer (one-times PBS and 1% FBS) and centrifuged for 10 min at 200 x *g*. Cells were incubated with antimouse CD80 FITC and CD86-APC antibodies for 1 h in dark. After washing with staining buffer, cells were fixed using 4% paraformaldehyde in dark for 20 min and ana-

lyzed the next day for maturation markers CD80 and CD86. Flow cytometry was conducted using a Beckman Coulter Cytomics FC 500 Flow Cytometer from core facility. For BMDC activation, BMDCs (~1 × 10^4) were plated in 96-well round bottom plates on day 6 and were pulsed with 0.5–1 mg of NPs for 24 and 48 h, respectively. Supernatants were collected at both time points and IL12 levels in the supernatants collected were measured using Mouse IL-12 p70 ELISA Ready-SET-Go reagent set from ebioscience as per manufacturer's instructions.

Syngeneic breast cancer BALB/c mice model

Mice were preimmunized intraperitoneally with CpG (600 µg/kg) and subsequently immunized with the respective NPs (as listed in Table 1) 7 days before tumor challenge. The required dose of NPs (6 mg) was calculated based on the encapsulation efficiency. Mice immunized with the CpG-NP-Tag NPs (n = 7) comprised the treatment group while the control group consisted of mice immunized with CpG-NP-Blank NPs (n = 7) and NP-Tag (n = 7). Seven days post NP immunization mice were challenged with 1 × 10^5 4T1 cells. Primary tumor size was monitored over the course of 21 days following tumor challenge. After sacrificing animals on day 21, spleens and primary tumors were procured for further studies (Figure 2).

Rate of tumor growth & animal weight

Tumor size and animal weight were measured until day 21 at different time intervals using vernier caliper and calibrated weighing balance, respectively. Tumor volume (mm^3) was calculated for all the animals using the below-mentioned formula [18]:

Tumor volume (mm^3) = $\pi/6$ (length × breadth × height).

Histological analysis of tumors

Tissues were fixed in 4% paraformaldehyde, embedded in optimum cutting temperature compound (Tissue-Tek, Sakura Fine-Tek, CA, USA) and sectioned using cryostat to obtain 5–8 µm thin sections. Frozen sections were stored at -80°C and used subsequently for immunofluorescence staining.

Hemoglobin estimation by Drabkin's reagent

To quantify the formation of functional vasculature in the tumor, the amount of hemoglobin (Hb) was measured using a Drabkin reagent kit 525 (Sigma, MO, USA) following the Drabkin and Austin method. Briefly, the excised tumors were chopped and homogenized in a Dounce homogenizer in presence of 0.5 ml deionized water and allowed to stand overnight at 4°C. The lysate was centrifuged at 5000 x *g* for 10 min and the supernatant was collected. 0.3 ml of each sample was mixed with 0.5 ml of Drabkin's reagent and allowed to stand for 15 min at room temperature. The absorbance was read at 540 nm by using Drabkin's reagent solution as blank. A standard curve was constructed by using known concentrations of Hb and the concentrations of the samples were obtained from the standard curve [19].

CD107α assay

CD107α assay was performed to evaluate CTL activity. For this assay, we followed the same study time

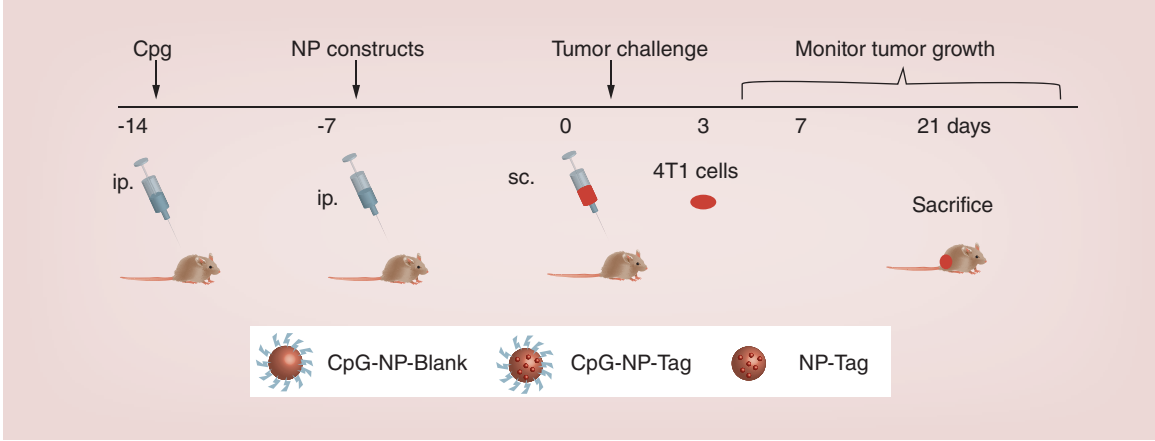

Figure 2. Schematic of the study timeline followed for the *in vivo* model. 5–6-week-old female BALB/c mice (n = 7) were preimmunized ip. with CpG 14 days before tumor challenge followed by ip. immunization (7 days after CpG preimmunization) with the respective groups of NPs. Mice were challenged sc. with 10^5 4T1 mammary carcinoma cells and the effect of NP immunization was evaluated on the rate of tumor growth and immune response for 21 days.

ip.: Intraperitoneally; NP: Nanoparticle; sc.: Subcutaneously; Tag: Tumor antigen.

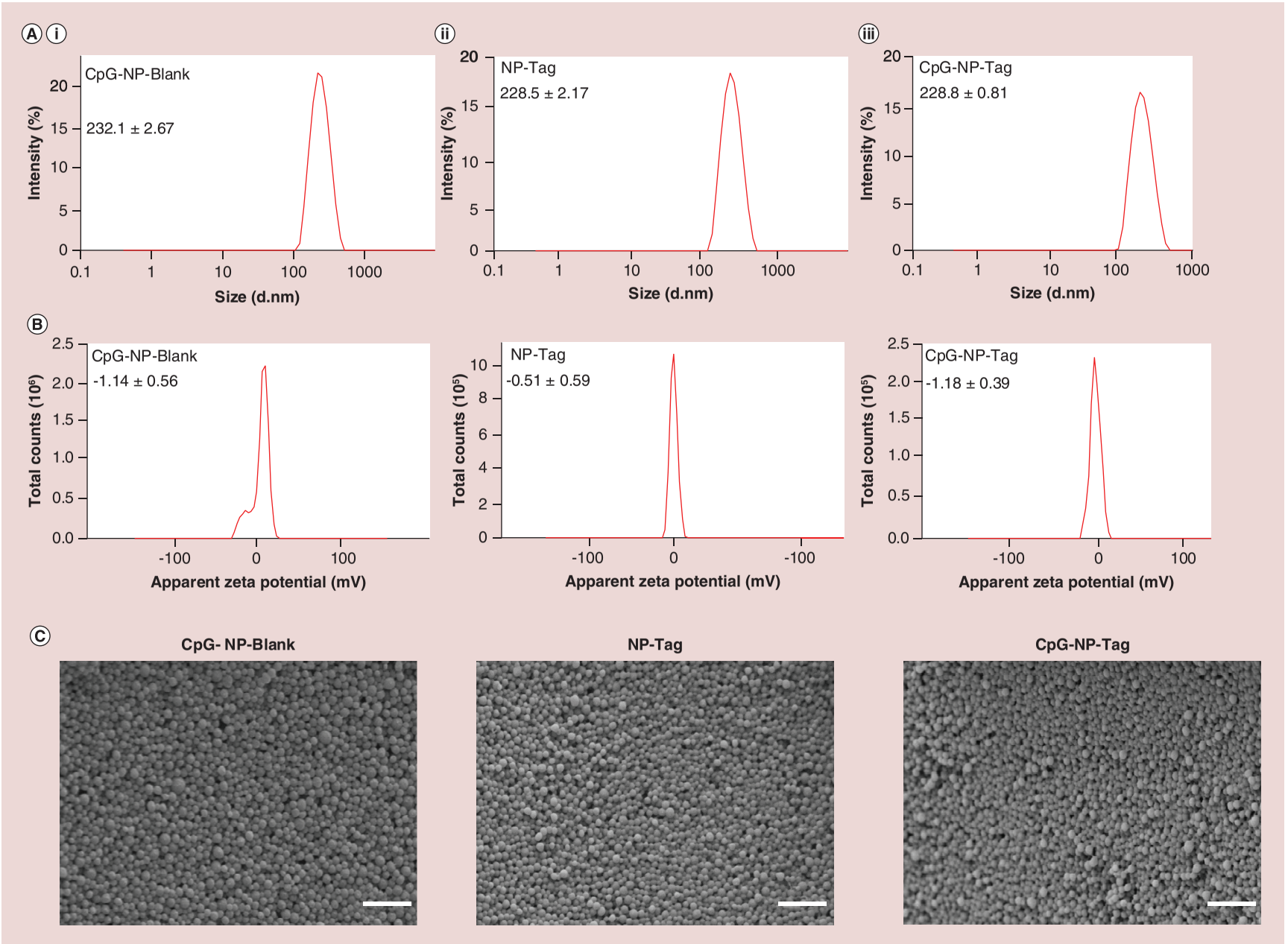

Figure 3. Characterization of nanoparticles. **(A)** Particle size distribution of CpG-NP-Blank **(i)**, NP-Tag **(ii)** and CpG-NP-Tag **(iii)** NPs obtained from dynamic light scattering measurements. **(B)** Surface zeta potential graphs for CpG-Blank, NP-Tag and CpG-NP-Tag NPs. **(C)** Scanning electron micrographs of CpG-Blank, NP-Tag and CpG-NP-Tag NPs (scale bar: 1 μm).
NP: Nanoparticle; Tag: Tumor antigen.

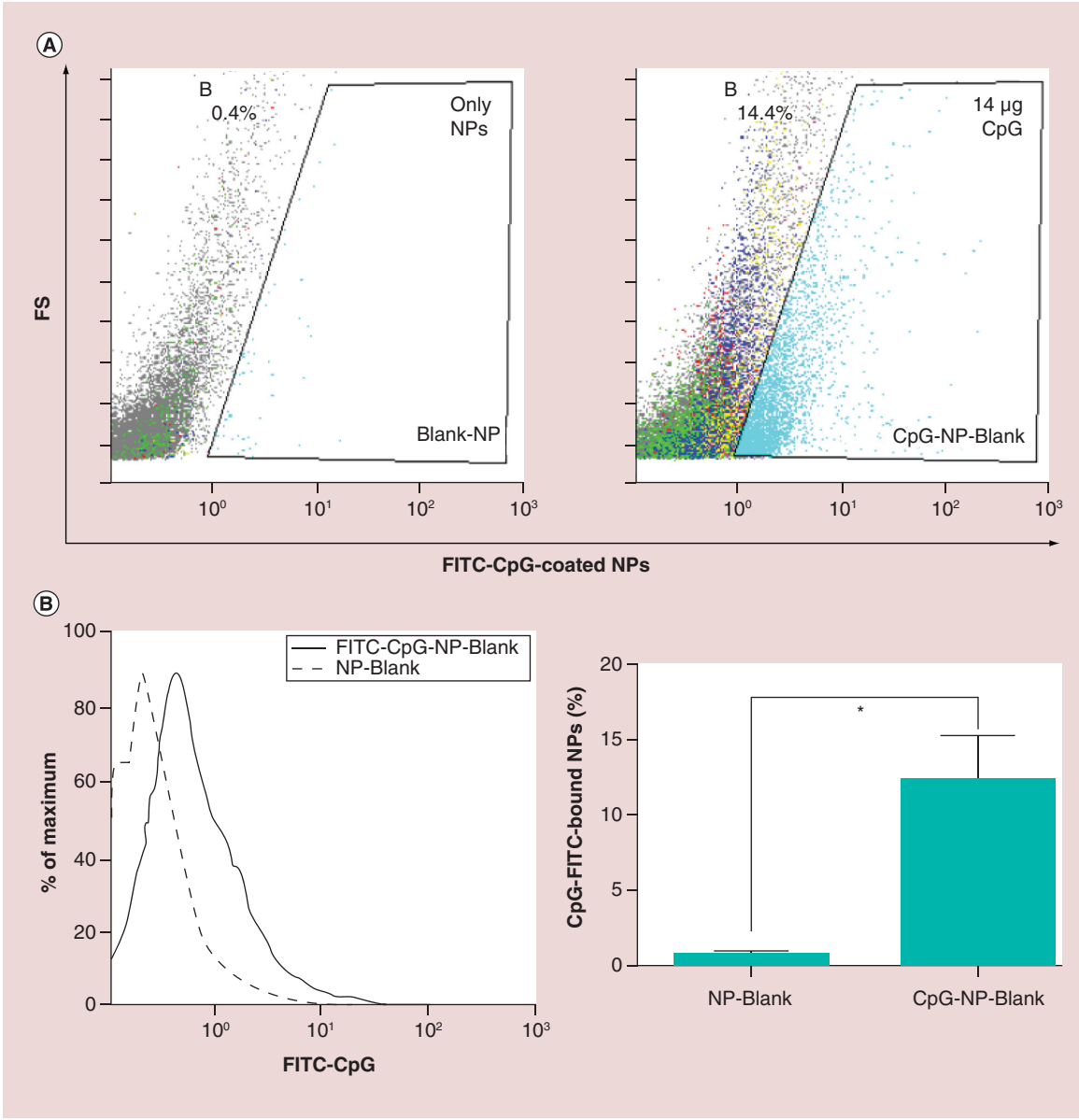

Figure 4. CpG ligand binding efficiency. Percentage of CpG-bound NPs. 1mg/ml of NPs were incubated with 14 µg of CpG-FITC and percentage of CpG-bound NPs was determined using flow cytometry. **(A)** Histograms of blank NPs and CpG-FITC-bound NPs (FITC-CpG-NP-Blank) indicating shift in fluorescence for the CpG-FITC-bound NPs. **(B)** Quantification of the ligand binding efficiency data obtained from flow cytometric measurements (*p < 0.05). NP: Nanoparticle.

line as mentioned before (Figure 2). After CpG pre-immunization and NP immunization, animals were sacrificed day 21 post-tumor challenge and spleens were harvested to obtain the splenocytes (effector cell population: E). For stimulation, splenocytes (primed *in vivo* due to NP immunization) stained with alexa 488 conjugated anti-CD107α were cocultured with target 4T1 cells (T) at different E: T (1:1; 5:1; 10:1; 20:1) ratios for 4–6 h. Flow cytometric analysis was conducted to measure the population of CD107a expressing CTLs.

Statistical analysis

GraphPad Prism 6 version and social science statistics software was utilized for analyzing biological assays. One-way ANOVA and unpaired Student's t test ($p < 0.05$) were used to analyze the *in vivo* and *ex vivo* data.

Results

Formulation & characterization of nanoparticles

CpG-NP-Tag NPs were prepared using our previously established modified double emulsion technique fol-

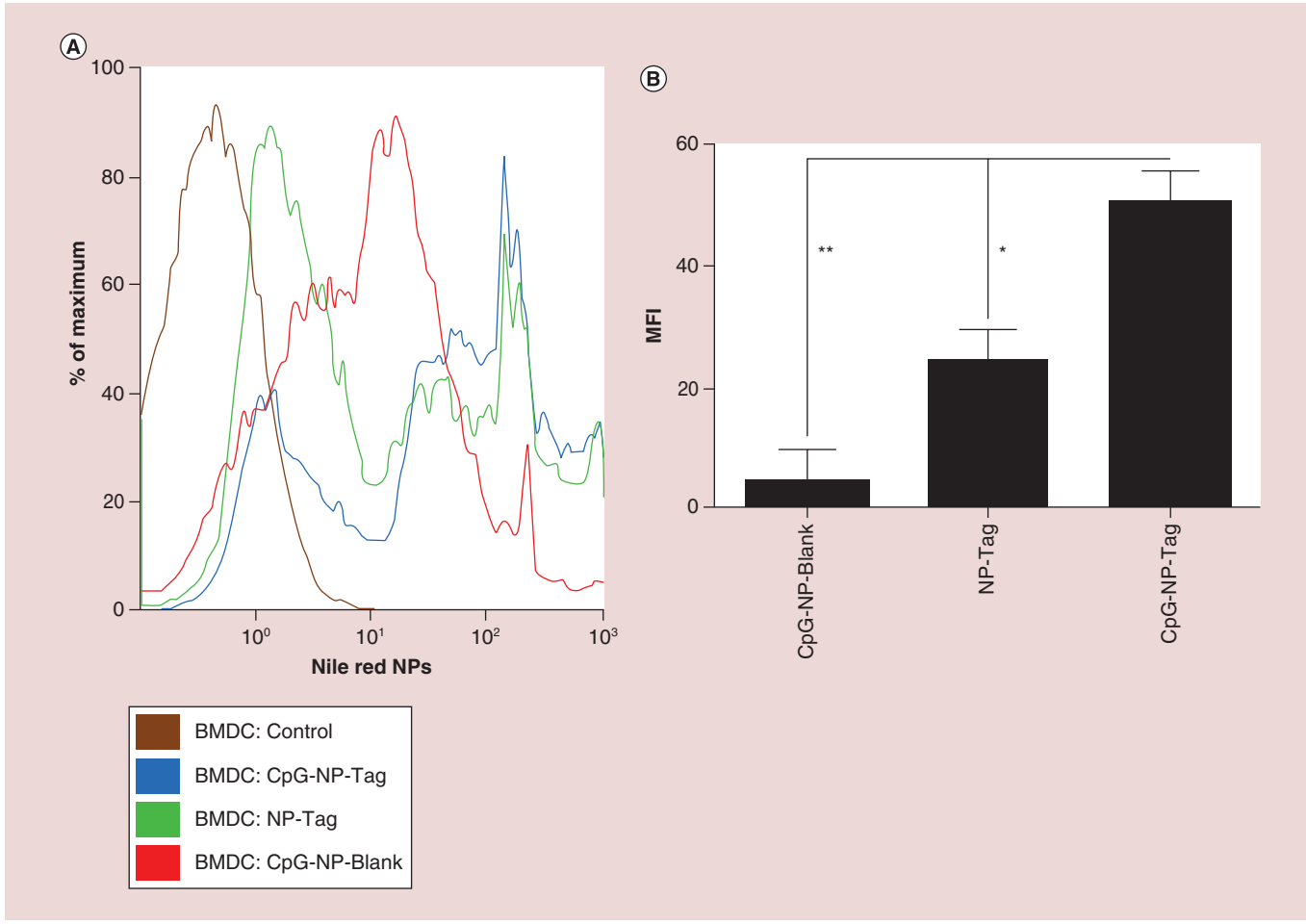

Figure 5. Uptake of nanoparticles in bone marrow-derived dendritic cells. (A) Percentage of BMDCs positive for the respective nile red-stained NPs as determined by flow cytometry. **(B)** MFI values indicating uptake of respective NPs in BMDCs.
*p < 0.05; **p < 0.01.
BMDC: Bone marrow-derived dendritic cell; MFI: Mean fluorescence intensity; NP: Nanoparticle; Tag: Tumor antigen.

lowed by solvent evaporation (Figure 1). Three groups of NPs were formulated as shown in Table 1. CpG-NP-Blank and NP-Tag NPs served as control groups for all our experiments along with the test CpG-NP-Tag formulation. We successfully incorporated Tag (membrane lysate of 4T1 tumor cells) in the NP core and docked CpG ligand on the surface employing BS3 crosslinker.

These NPs were characterized for particle size, PDI, zeta potential, surface morphology, CpG ligand binding efficiency and Tag encapsulation efficiency. The particle size of noncoated NP-Tag particles and coated CpG-NP-Blank and CpG-NP-Tag NPs were found to be 227.3 ± 0.07 nm, 230.6 ± 0.78 nm and 229.2 ± 0.71 nm, respectively (Figure 3A & Table 1). Surface zeta potential was found to be, -1.14 ± 0.56 mV for CpG-NP-Blank, -0.51 ± 0.59 for NP-Tag and -1.18 ± 0.39 for CpG-NP-Tag NPs (Figure 3B & Table 1). PDI and encapsulation efficiency for the respective NP formulations are listed in Table 1. Scanning electron microscopy (SEM) images of the particles confirmed the particle size as well as morphology. Particles were found to be uniform in size, spherical and nonagglomerated with smooth surface (Figure 3C). The CpG ligand binding efficiency tested by flow cytometry was found to be around 12–14% (Figure 4A & B).

Ex vivo immunostimulatory efficacy of CpG-NP-Tag NPs

Dendritic cell uptake & intracellular localization

The uptake of NPs by APCs was determined in BMDCs obtained from female Balb/c mice as described in BMDC NP uptake and Intracellular Localization. The percentage of cells with NPs as well as the Mean Fluorescence Intensity data were collected from this experiment. Percent of cells that had engulfed CpG-NP-Tag was found to be slightly greater than control NP-Tag NPs and significantly greater than control CpG-NP-Blank NPs (Figure 5A). Mean fluorescence intensity data indicated CpG-NP-

Tag NPs had significantly higher uptake as compared with the other NP constructs ($p = 0.0057$) (Figure 5B). CpG ODN is a TLR9 ligand that is expressed intracellularly in the endocytic compartment. Thus, to check endosomal localization of the CpG-coated NPs (CpG-NP-Blank and CpG-NP-Tag) we used confocal microscopy. We pulsed the BMDCs on day 7 with the respective nile red stained NP formulations for 1 h and processed the cells for immunocytochemistry as described in BMDC NP uptake and Intracellular Localization. Confocal images revealed that CpG-NP-Blank and CpG-NP-Tag NPs (red) were largely accumulated in endosomal compartment (green) as compared with noncoated ones (NP-Tag) (Figure 6A). Percent colocalization calculation also indicated higher number of nile red stained coated (CpG-NP-Blank and CpG-NP-Tag) particles (red) colocalized (yellow) with the early endosomal compartment (green) (Figure 6A & B). To negate any differences as a result of Tag, additional studies using JAWSII cell line also demonstrated significant differences in the uptake and intracellular localization for coated (CpG-NP-Blank) and compared with uncoated (NP-Blank; refer to Supplementary Figures S4 & S5).

BMDC activation & maturation

DC-based immune induction involves pathogen recognition and uptake, migration, activation and maturation [20]. As a potential vaccine delivery system NPs must be engulfed in sufficient amounts leading to subsequent activation and maturation of DCs. After evaluating the uptake, we determined the capability of NPs to induce DC activation and maturation by measuring the expression of costimulatory surface maturation markers CD80/86 and cytokine (Interleukin-12) IL-12. BMDCs were pulsed with respective groups of NPs for 48 h and the cells were processed and tested for maturation markers CD80/86 by flow cytometry. Percent of CD80 and CD86 positive cells were calculated and it was found to be significantly higher in case of CpG-NP-Tag pulsed BMDCs as compared with controls ($p < 0.0001$) (Figure 7A & B). Supernatants were collected from cultures to determine IL-12 cytokine production from NP-pulsed BMDCs as described in BMDC Maturation and Activation. CpG-NP-Tag and CpG-NP-Blank-pulsed BMDCs secreted significantly high levels of IL-12 as compared with noncoated NP-Tag NPs ($p < 0.0001$) (Figure 7C) while no significant dif-

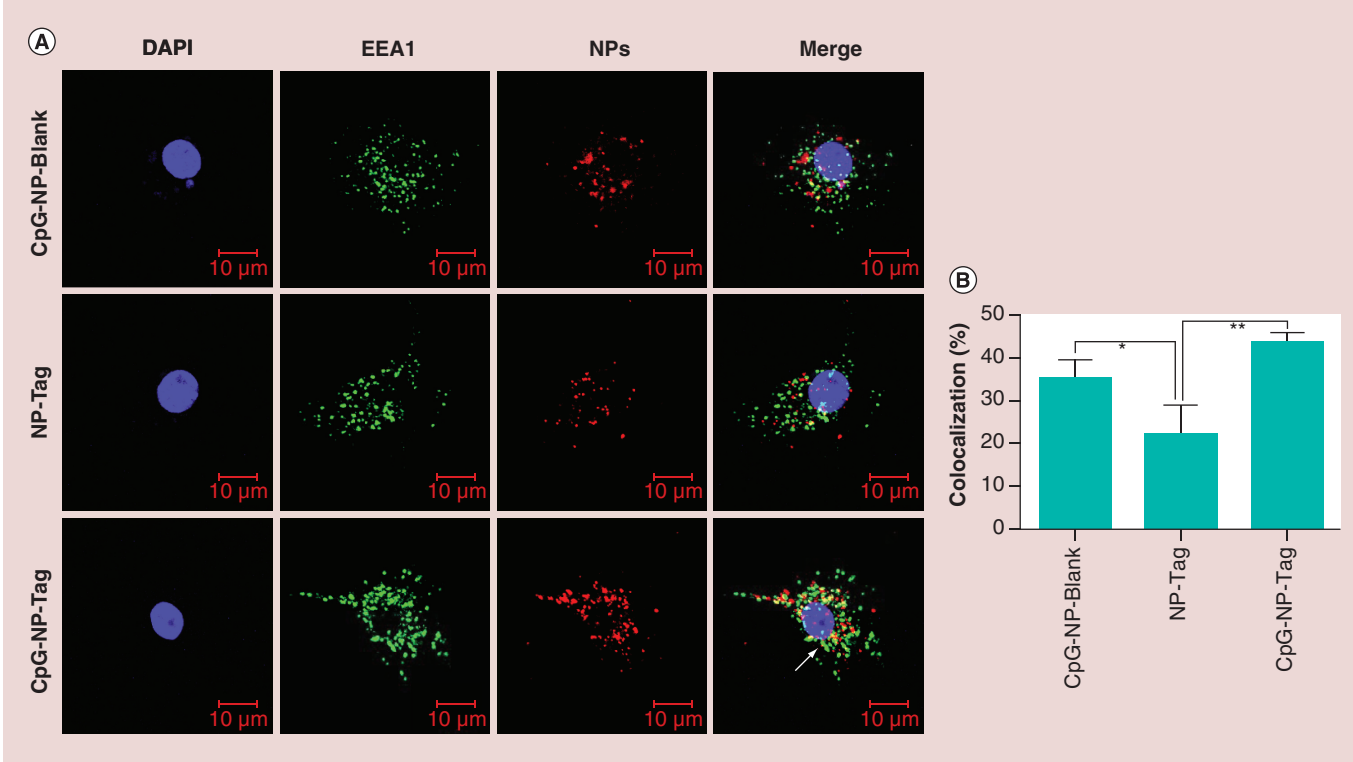

Figure 6. Nanoparticle bone marrow-derived dendritic cells intracellular localization. **(A)** Representative images (40-times) showing the endosomal (green) colocalization (yellow) of the different nile red-stained NPs in bone marrow-derived dendritic cells. **(B)** Percentage colocalization determined in NP-pulsed bone marrow-derived dendritic cells. Imaged show nile red-stained particles (red) colocalized (yellow) with the early endosomal compartment (green; EEA1).
*$p < 0.05$; **$p < 0.01$.
NP: Nanoparticle; Tag: Tumor antigen.

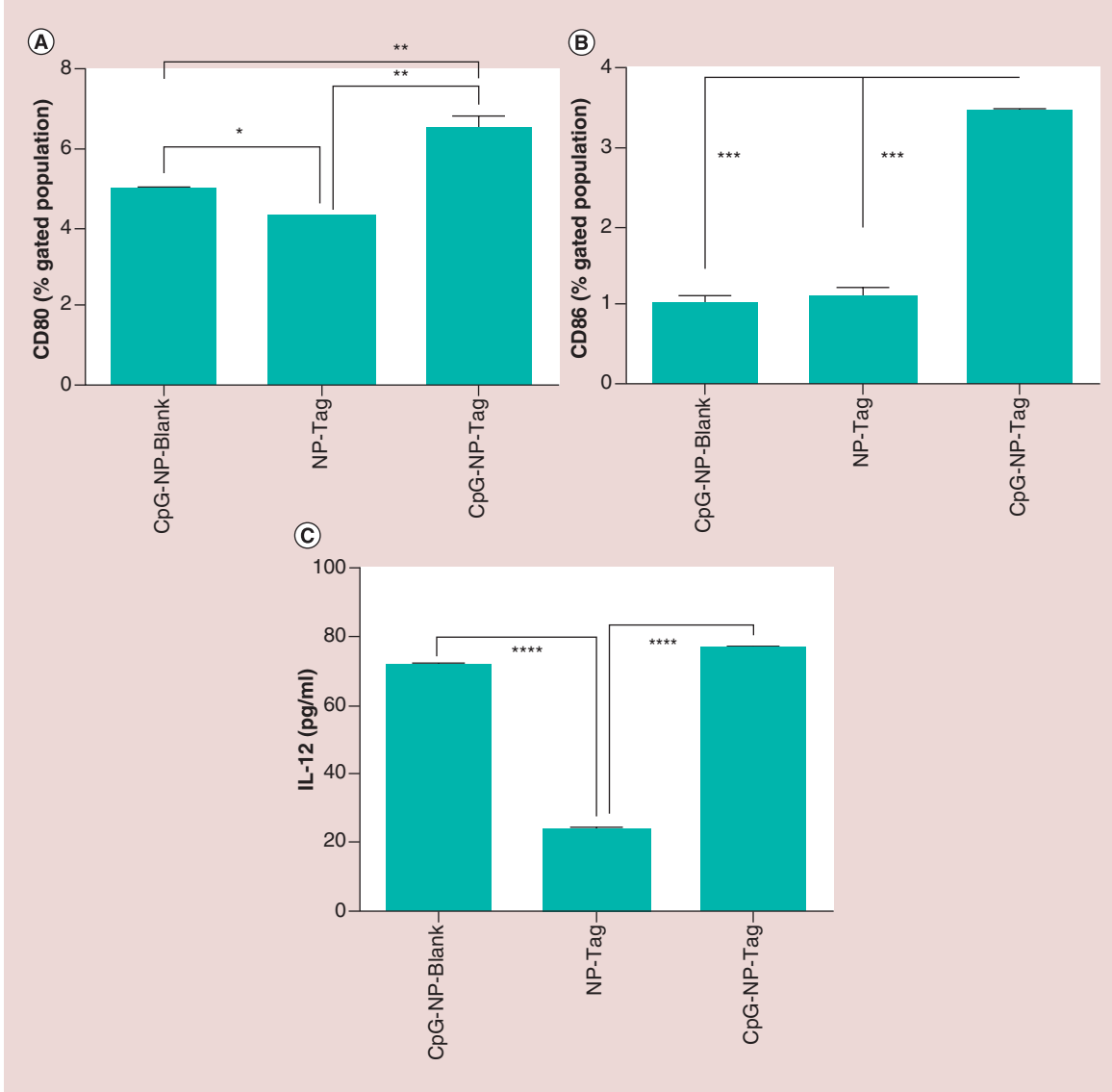

Figure 7. Effect of nanoparticles on bone marrow-derived dendritic cell activation and maturation. (A) Percentage of NP-pulsed bone marrow-derived dendritic cells (BMDCs) expressing CD80. **(B)** Percentage of NP-pulsed BMDCs expressing CD86. **(C)** IL12 cytokine levels (pg/ml) in supernatants collected from NP-pulsed BMDCs post-48 h measured by ELISA.
****p < 0.0001.
NP: Nanoparticle; Tag: Tumor antigen.

ference was observed between the CpG-NP-Blank and CpG-NP-Tag NPs (coated NPs).

In vivo Immunoregulatory role of CpG-NP-Tag NPs

Our previous studies show CpG preimmunization preceding CpG-NP-Tag NP immunization promotes enhanced IFN-γ production and $CD4^+$/$CD8^+$ tumor T-cell infiltration [9]. Thus, we utilized a similar CpG preimmunization scheme for our current studies as described in 'Generation of bone marrow-derived dendritic cells'. Syngeneic breast Cancer BALB/c Mice Model and Figure 2. We monitored tumor growth using vernier caliper (Rate of Tumor Growthand Animal Weight) at different time points until day 21 and found attenuation of tumor growth (Supplementary Figure S1) as in our previously published studies [9]. After euthanasia of mice, tumors, spleens and serum were collected for further analysis of immunostimulatory functions of CpG-NP-Tag NPs.

Angiogenic activity

Angiogenic activity is a hallmark of tumor aggressiveness. Prior to tumor excision, solid tumors were visually inspected for vascularity. Tumors of control-treated mice

demonstrated dense vascularization as compared with tumor from CpG-NP-Tag-vaccinated mice (Figure 8A).

To confirm and quantify the angiogenic activity the excised tumors were subjected to biochemical analysis using Drapkins reagents to test the Hb levels which serve as an indirect marker of angiogenesis. CpG-NP-Blank as well as NP-Tag control tumors as expected showed high Hb levels as compared with CpG-NP-Tag tumors ($p = 0.03$) (Figure 8B). In addition, excised tumors from representative control and CpG-NP-Tag vaccinated mice were fixed in 4% paraformaldehyde and embedded in optimum cutting temperature and frozen sections were used for further investigation. Immunofluorescence images for CD31 or platelet endothelial cell adhesion molecule, a known angiogenesis marker, indicated a significantly high degree of angiogenesis in case of control CpG-NP-Blank as well as NP-Tag tumors relative to CpG-NP-Tag tumors ($p = 0.0011$) (Figure 9A & B). We also determined the local production of cytokine IFN-γ which is known for its antiangiogenic activities via intracellular staining in the tumor sections (Supplementary Figure S2). We observed low levels of IFN-γ in tumor microenvironment correlating to high Hb levels as well as higher CD31 staining in case of control groups while high local production of IFN-γ was seen in CpG-NP-Tag tumors which correlating to low Hb levels and CD31 staining (Figures 8B, 9A, 9B & Supplementary Figure S2).

Cytotoxic T-cell activity

$CD8^+$ T cells are the major effector cell population involved in tumor cell killing. To evaluate the CTL

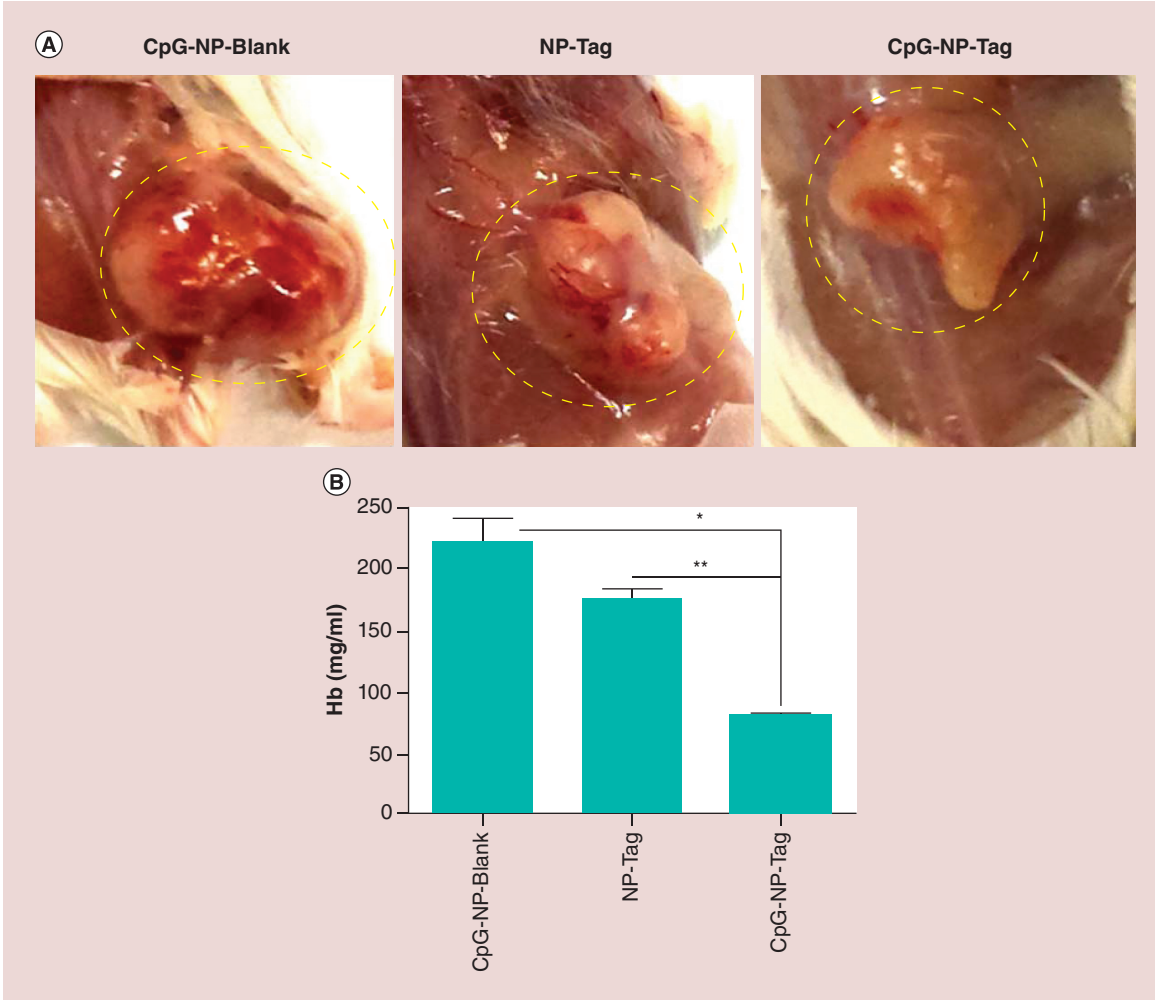

Figure 8. Effect of nanoparticle immunization on tumor vasculature. (A) Representative images of blood vessel vascularization surrounding the primary tumor tissue in tumor-bearing mice prior to resection of tumor. **(B)** Hb estimation for quantification of blood vascularization (angiogenesis) in tumors harvested from NP-immunized mice.
*$p < 0.05$; **$p < 0.01$.
Hb: Hemoglobin; NP: Nanoparticle; Tag: Tumor antigen.

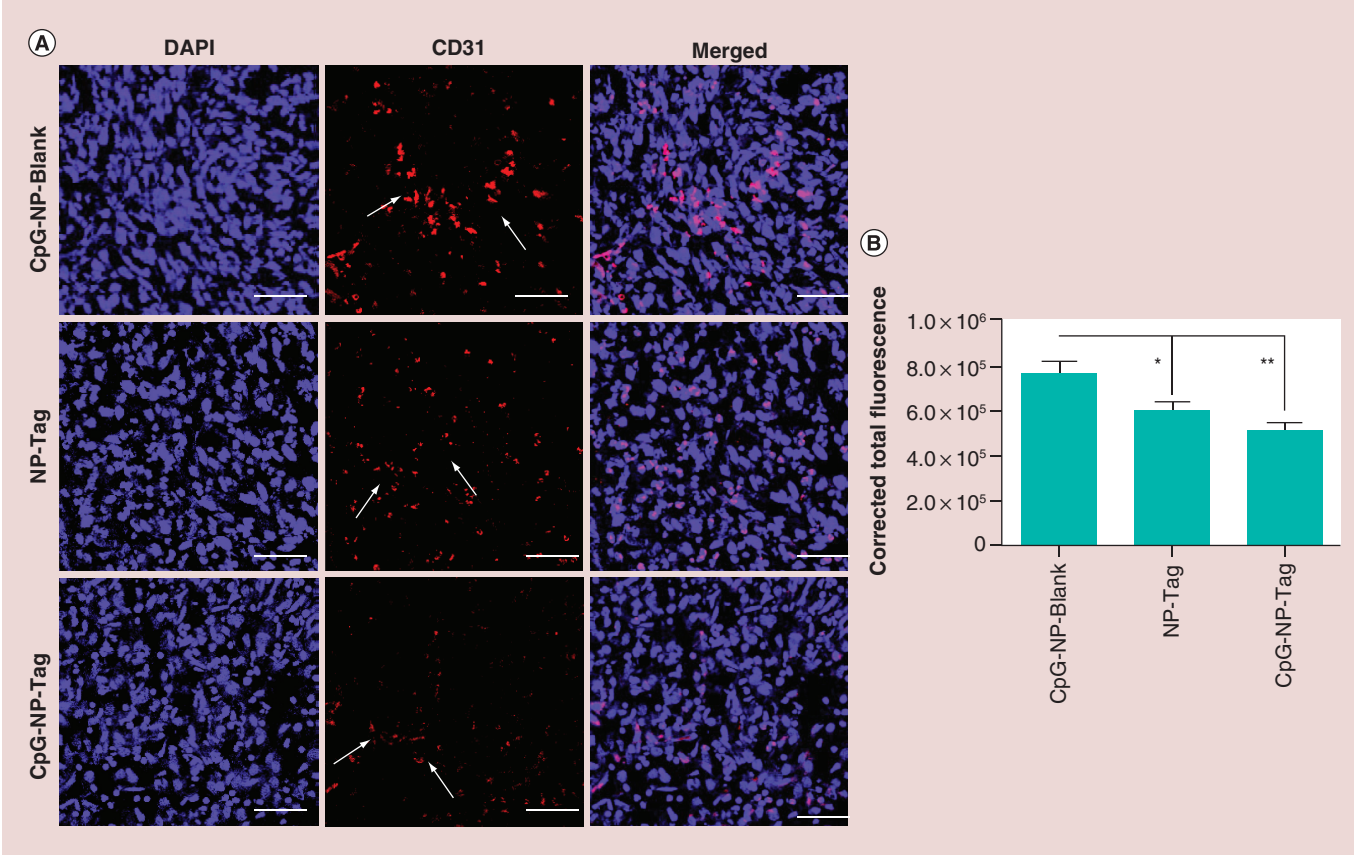

Figure 9. Effect of nanoparticle immunization on angiogenesis. (A) Representative images (40-times) of CD31-stained tumor tissues sections showing the angiogenic blood vascularization. **(B)** Quantitative analysis indicating angiogenic activity surrounding the tumor tissue harvested from the different groups analyzed using NIH ImageJ software.
*p < 0.05; **p < 0.01.
NP: Nanoparticle; Tag: Tumor antigen.

activity of these T lymphocytes we used CD107α assay. For this experiment, we used the entire splenocytes population obtained from immunized tumor bearing mice and cocultured it with target 4T1 tumor cells (CD107α Assay). The experiment was conducted at different effector: target ratios and CTL activity was quantified further using flow cytometry. Results from the killing assay indicate that splenocytes from the CpG-NP-Tag immunized mice displayed higher percentage of $CD107a^+$ population as compared with control mice implying enhanced CTL function (Figure 10).

Discussion

One of the challenges in using NP-based technology in cancer immunotherapy is the development of a suitable delivery vehicle which is clinically safe and toxic. Multifunctional nanosystems (dendrimers, polymeric NPs, metallic NPs) allows use of different technologies (surface attachment, encapsulation, labeled NPs) for site-specific, simultaneous or sequential delivery of multiple components (Ags, adjuvants, peptides, tracking agents/dyes) to APCs, particularly DCs as they are key immune-based regulators [1,11]. PLGA is an US FDA-approved biodegradable polymer that has been employed in several studies to fabricate microparticle or NPs [6,7]. These NPs can encapsulate a variety of biologically active compounds ranging from anticancer drugs to peptides or hormones. Many such products are on the market or under clinical investigation [21]. Various antigenic substances (proteins, peptides, plasmid DNA, viruses) have been successfully delivered using PLGA particles and therefore are good candidates for vaccine delivery. Our group recently published a study demonstrating the antitumor effects of PLGA-based CpG-coated Tag encapsulated (CpG-NP-Tag) NPs after *in vivo* administration in a prophylactic setting [9]. In the current manuscript, we show *ex vivo* studies using CpG-NP-Tag NPs with BMDCs to identify the feasibility of such construct on antitumor action at the level of the APC.

The studies in this manuscript mainly focus on delineating the mechanism of antitumor action of CpG-NP-Tag NPs. Protecting the encapsulated cargo from degradation prior to targeted recognition by DCs would optimize the induction of anti-tumor immune responses.

The physical and chemical composition of prospective NP constructs is of highest priority to ensure that NPs are primarily engulfed by phagocytic DCs preventing Ag dissemination into systemic circulation [15,22]. Previous studies have shown that PLGA NPs smaller than 500 nm in size are preferentially taken by DCs and more effective in generating CTL responses *in vivo* relative to microparticles (>2 µm) [23]. We have successfully engineered CpG-coated Tag containing PLGA NPs (CpG-NP-Tag) using the solvent evaporation technique resulting in a particle size ranging from 200 to 230 nm (Figures 1, 3A & Table 1) which is desirable for preferential DC uptake as compared with macrophages and evaluated the effect of CpG-NP-Tag NPs on BMDCs *ex vivo* [23,24].

Surface zeta potential, morphology and particle size of colloidal nanosytems has a major impact on cellular uptake as well as intracellular trafficking. Specifically, spherical negatively charged particles are avidly phagocytosed at higher rates compared with neutral and highly positive charged particles [25,26] which is linked to the receptive negative charge of cellular membranes [27,28]. Spherical-coated particles (CpG-NP-Tag and CpG-NP-Blank) were slightly more negative as a consequence of negatively charged CpG-DNA than uncoated ones (Figures 3B, 4B & Table 1). We were able to attain encapsulation efficiency of ~38%. Although effective, such modest encapsulation efficiency was likely attributed to the hydrophilic nature of the Tag (4T1 membrane lysate in RIPA buffer). A PDI close to zero is optimal as it indicates uniform size distribution [29]. The PDI of the prepared particles was in the desirable range of 0.13–0.16 (Table 1). Ligand binding efficiency quantified using flow cytometry was found to be around 12–14% (Figure 4). In total, this construction methodology holds promise as a proof of concept for NP-based design targeting DCs.

The role of DCs in promoting CTL-based immunity is well established [12–14,30,31]. The development of protocols for isolation and *in vitro* culture of DCs has revolutionized the field of DC-based vaccines. Two main strategies are currently accepted with respect to DC vaccination models: *ex vivo* loading and *in vivo* targeting. Our results demonstrate the efficacy of CpG-NP-Tag NPs to serve as potential candidates for *ex vivo* based DC vaccines. Sufficient uptake of NPs is a prerequisite to render effective DC-based immune responses. We found that uptake of CpG-NP-Tag NPs was significantly higher in BMDCs compared with CpG-NP-Blank or NP-Tag NPs (Figure 5). We attribute the higher uptake to the presence of both CpG and Tag. We also checked the intracellular localization of the respective NPs. We found greater percent co-localization within the endosomal compartment for CpG-coated NPs (CpG-NP-Blank and CpG-NP-Tag) than the uncoated ones (NP-Tag) (Figure 6). We believe CpG being a TLR9 ligand will preferentially route the coated NPs to endosome where the TLR9 receptors are located. To confirm DC activation and function crucial for transport of processed Ag-loaded MHC complexes to cell surface we probed for maturation markers (CD80/B7–1 and CD86/B7–2) as well as IL-12 secretion. The transport of MHC-peptide complex to cell surface is accompanied with increased expression of costimulatory molecules (CD80/86). These are known to play a key role in the amplification of T-cell receptor signaling and thereby T-cell activation [32]. Our studies indicated a higher percentage of BMDCs expressing CD80 and CD86 molecules for CpG-NP-Tag-pulsed BMDCs compared with control groups (Figure 7). Function of DCs was evaluated by comparing IL-12 secretion among the NP-pulsed BMDCs. IL-12 is naturally produced by DCs in response to antigenic stimulation and typically aids in the growth, function and CTL activity of $CD8^+$ T lymphocytes. IL-12 is also known to have antiangiogenic role which it mediates via increasing secretion of IFN-γ. Interestingly, IL-12 levels were seen to be higher in case of BMDCs pulsed with coated NPs (CpG-NP-Blank and CpG-NP-Tag) as compared with uncoated ones (NP-Tag) (Figure 7C). We believe that this might be due to the presence of CpG, which promoted IL-12 secretion. Although presence of CpG might facilitate increased endosomal localization and IL-12 secretion (as seen in case of CpG-NP-Blank NPs), incorporating

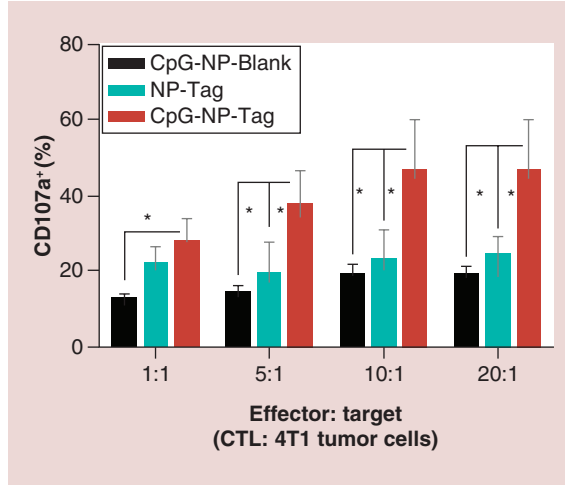

Figure 10. Quantification of cytotoxic $CD8^+$ T lymphocyte activity. CTL activity was measured using CD107α assay. Splenocytes (primed *in vivo* due to NP immunization) obtained from tumor-bearing mice at day 21 were stained with alexa 488-conjugated anti-CD107α and subsequently cocultured with target 4T1 cells (T) at different E: T (1:1; 5:1; 10:1; 20:1) ratios for 4–6 h. Flow cytometric analysis was conducted to measure the population of CD107α-expressing CTLs. *$p < 0.05$.
CTL: Cytotoxic T lymphocyte; NP: Nanoparticle; Tag: Tumor antigen.

Tag in the formulation (as in CpG-NP-Tag) is essential in avoiding nonspecific immune responses and generating tumor-specific T-cell responses. Thus, these results demonstrate that CpG-NP-Tag NPs could be used for *ex vivo* targeted DC vaccines.

IFN-γ is an extensively studied cytokine in vaccine therapy. This cytokine is known to have a protective role and mediate its antitumor effects via affecting tumor growth/survival cell proliferation, inhibiting angiogenesis and enhancing innate and adaptive immune functions [33]. The studies published previously by Kokate *et al.* portray the proof of concept indicating the immunostimuaory potential of CpG-NP-Tag NPs to induce antitumor effects [9] (evident from the increased tumor $CD4^+/CD8^+$ T-cell infiltration and local IFN-γ production), while in the current study we show that tumor inhibiting properties (Supplementary Figure S1) may be due to an antiangiogenic effect (possibly mediated via IFN-γ) and enhanced CTL function in CpG-NP-Tag NP-immunized mice (Figures 8–10). Interestingly, these results concerted with the high IFN-γ in our previous studies (Supplementary Figure S2). Thus, there is likelihood that the antiangiogenic effect seen may be mediated due to local production of IFN-γ in the tumor microenvironment. IFN-γ also originally known as 'macrophage activating factor' is an important stimuli for the activation of macrophages which further induce direct antitumor effects as well as upregulates Ag presentation [34]. Additionally, IFN-γ polarizes macrophages toward the inflammatory M1 phenotype thus helping in tumor eradication [35]. We were able to demonstrate a significant increase in macrophage infiltration in CpG-NP-Tag tumors as compared with control tumors (refer to Supplementary Figure S3). Further investigation in this direction will be needed to characterize the phenotype of these infiltrating macrophages.

Collectively, all the studies conducted in this project *ex vivo* as well as *in vivo* delineate CpG-NP-Tag NPs facilitate stimulation and activation of DCs, attenuation of breast tumor growth and angiogenesis by enhancing local IFN-γ production and CTL-mediated immune responses thus indicating the dual role (*in vivo* and *ex vivo*) CpG-NP-Tag in vaccination models.

Conclusion

From the studies conducted with 'bacteriomimetic' NPs (CpG-NP-Tag) until now we show the dual use of these NPs – *ex vivo* to increase the efficacy of DCs by inducing the expression of maturation markers (CD80/CD86) as well as IL-12 secretion which in turn will aid T-cell responses and *in vivo* to attenuate tumor growth, proliferation, angiogenesis and to induce apoptotic death of tumor cells possibly due to the induction of optimal antitumor CTL responses. Based on these results, it is hard to sideline the plausibility that DCs might orchestrate the *in vivo* effects of CpG-NP-Tag NPs. Thus, we plan to conduct some more experiments in future in order to investigate role of CpG-NP-Tag in the *in vivo* and *ex vivo* targeting of DCs.

Future perspective

DC-based vaccination schemes have been successful in delivering vaccine Ag to lymphatic tissues and enhance CTL response. However, DC vaccines have shown poor clinical efficacy due to insufficient Ag uptake by DCs. Therefore, to improve Ag uptake, NP-based delivery system have been explored. Studies reported that particulate PLGA vaccines could enhance uptake of Ag and adjuvants by DCs resulting in improved immune responses. Thus, fabrication of NPs with 'danger signals' such as TLR agonists or pathogen-associated molecular patterns on surface could activate APCs and stimulate NP uptake. Multivalent presentation of TLR agonists (such as CpG-ODN) or pathogen associated molecular patterns through surface modifications will render repetitive presentation of pathogens 'mimicking' infection and promoting better immune response through receptor cross linking and immune cell activation. Studies conducted with PLGA-based CpG-NP-Tag NPs are of translational value since these NPs portray potential to be candidate DC vaccine carriers could be in future optimized for successful *in vivo* DC targeting.

Acknowledgements

The authors would like to thank Dr A Darehshouri from Electron Microscopy Core Facility, UT Southwestern Medical Center for help with the SEM imaging.

Financial & competing interests disclosure

This research was supported in part by National Institute on Minority Health and Health Disparities Grant 1P20 MD006882 (to JK Vishwanatha), Department of Molecular and Medical Genetics at UNTHSC and Predoctoral Bridge Funding Grant (R16138) from UNTHSC. The authors have no other relevant affiliations or financial involvement with any organization or entity with a financial interest in or financial conflict with the subject matter or materials discussed in the manuscript apart from those disclosed.

No writing assistance was utilized in the production of this manuscript.

Ethical conduct of research

The authors state that they have obtained appropriate institutional review board approval or have followed the principles outlined in the Declaration of Helsinki for all human or animal experimental investigations. In addition, for investigations involving human subjects, informed consent has been obtained from the participants involved.

Executive summary

Polymeric nanoparticles: delivery system & immune potentiator

- Polymeric poly (D, L-lactide-co-glycolide) nanoparticles (NPs) have offered new avenues for engineering of cancer vaccines.
- Surface functionalization of tumor antigen (Tag) encapsulated poly (D, L-lactide-co-glycolide) NPs with immune stimulants such as CpG-ODN enhances the immune boosting capacity of such NPs.

Formulation & characterization of poly (D, L-lactide-co-glycolide) CpG-NP-Tag 'bacteriomimetic' NPs

- CpG-coated Tag containing 'bacteriomimetic' NPs (CpG-NP-Tag) can be formulated using well-established w/o/w double emulsion method employing solvent evaporation technique and further characterized for optimum particle size, polydispersity index, surface zeta potential, encapsulation efficiency and CpG ligand binding efficiency.

Immunoregulatory & antiangiogenic role of CpG-NP-Tag NPs

- Bone marrow-derived dendritic cells (DCs) show enhanced uptake and intracellular endosomal localization of CpG-NP-Tag NPs.
- CpG-NP-Tag NP treatment results in the upregulation of maturation markers CD80/86 and increased IL-12 secretion in bone marrow-derived DCs.
- CpG-NP-Tag NP immunization upregulates the CD 107α expression on killer T cells.
- CpG-NP-Tag NP immunization significantly reduces tumor growth rate and angiogenesis *in vivo* in a prophylactic setting.

Conclusion

- CpG-NP-Tag NPs promote DC maturation and activation crucial for the functioning of DC-based cancer vaccines.
- CpG-NP-Tag NPs attenuate tumor growth, angiogenesis and enhance cytotoxic T-lymphocyte function.
- CpG-NP-Tag NPs could serve as a platform for the development of DC-based immunotherapeutic interventions.

References

Papers of special note have been highlighted as:
• of interest; •• of considerable interest

1 Conniot J, Silva JM, Fernandes JG *et al.* Cancer immunotherapy: nanodelivery approaches for immune cell targeting and tracking. *Front. Chem.* 2, 105 (2014).

2 Cruz LJ, Tacken PJ, Rueda F, Carles Domingo J, Albericio F, Figdor CG. Targeting nanoparticles to dendritic cells for immunotherapy. *Meth. Enzymol.* 509, 143–146 (2012).

• **Provides useful information about targeted delivery of nanoparticle vaccine constructs to dendritic cells (DCs) leading to enhancement of vaccine potency and induction of strong cytotoxic T-cell response.**

3 Savla R, Ivanova V, Minko T. Nanoparticles in the development of therapeutic cancer vaccines. *Pharm. Nanotechnol.* 2(1), 2–22 (2014).

• **Details how nanoparticles could be modified based on shape, surface charge, size and composition for immune cell targeting as well as multiple antigen/adjuvant encapsulation and codelivery to elicit a robust–specific antitumor immune response.**

4 Müller L, McArdle S, Derhovanessian E *et al.* Current strategies for the identification of immunogenic epitopes of tumor antigens. In: *Immunotherapy of Cancer.* Humana Press, NY, USA, 21–44 (2006).

5 Akagi T, Baba M, Akashi M. Biodegradable nanoparticles as vaccine adjuvants and delivery systems: regulation of immune responses by nanoparticle-based vaccine. In: *Polymers in Nanomedicine.* Springer-Verlag, Berlin, Heidelberg, 31–64 (2012).

6 Krishnamachari Y. PLGA microparticle based vaccine carriers for an improved and efficacious tumor therapy. Chapter 1, 1–16 (2011). http://ir.uiowa.edu/etd/2922/

7 Krishnamachari Y, Geary SM, Lemke CD, Salem AK. Nanoparticle delivery systems in cancer vaccines. *Pharm. Res.* 28(2), 215–236 (2011).

8 Krishnamachari Y, Salem AK. Innovative strategies for co-delivering antigens and CpG oligonucleotides. *Adv. Drug Deliv. Rev.* 61(3), 205–217 (2009).

•• **Discusses novel strategies to codeliver tumor antigen (Tag) and CpG-ODN adjuvant to same antigen (Ag)-presenting cell in order to increase uptake by Ag-presenting cells which can result in Ag-specific immune responses greater than administration of Tag alone.**

9 Kokate RA, Thamake SI, Chaudhary P *et al.* Enhancement of anti-tumor effect of particulate vaccine delivery system by'bacteriomimetic'CpG functionalization of poly-lactic-co-glycolic acid nanoparticles. *Nanomedicine* 10(6), 915–929 (2015).

10 Cruz LJ, Tacken PJ, Fokkink R *et al.* Targeted PLGA nano-but not microparticles specifically deliver antigen to human dendritic cells via DC-SIGN *in vitro*. *J. Control. Release* 144(2), 118–126 (2010).

• **Shows how antibody-coated targeted poly (D, L-lactide-co-glycolide) (PLGA) nanoparticles interact specifically with DCs over microparticles as well as the degradation kinetics of PLGA-encapsulated Ag in DCs.**

11 Klippstein R, Pozo D. Nanotechnology-based manipulation of dendritic cells for enhanced immunotherapy strategies. *Nanomedicine* 6(4), 523–529 (2010).

12 Palucka K, Banchereau J. Cancer immunotherapy via dendritic cells. *Nat. Rev. Cancer* 12(4), 265–277 (2012).

13 Palucka K, Banchereau J, Mellman I. Designing vaccines based on biology of human dendritic cell subsets. *Immunity* 33(4), 464–478 (2010).

14 Palucka K, Ueno H, Zurawski G, Fay J, Banchereau J. Building on dendritic cell subsets to improve cancer vaccines. *Curr. Opin. Immunol.* 22(2), 258–263 (2010).

15 Hamdy S, Haddadi A, Hung RW, Lavasanifar A. Targeting dendritic cells with nano-particulate PLGA cancer vaccine formulations. *Adv. Drug Deliv. Rev.* 63(10), 943–955 (2011).

•• **The main goal of this review is to provide insight on the application of PLGA nanoparticles as cancer vaccine delivery vehicles and emphasize their potential for future development of immune-based therapeutic interventions.**

16 Manish M, Rahi A, Kaur M, Bhatnagar R, Singh S. A single-dose PLGA encapsulated protective antigen domain 4 nanoformulation protects mice against Bacillus anthracis spore challenge. *PLoS ONE* 8(4), e61885 (2013).

17 Kim B, Jones HP. Epinephrine-primed murine bone marrow-derived dendritic cells facilitate production of IL-17A and IL-4 but not IFN-γ by $CD4^+$ T cells. *Brain Behav. Immun.* 24(7), 1126–1136 (2010).

18 Feldman JP, Goldwasser R, Mark S, Schwartz J, Orion I. A mathematical model for tumor volume evaluation using two-dimensions. *J. Appl. Quant. Methods* 4, 455–462 (2009).

19 Drabkin DL, Austin JH. Spectrophotometric studies II. Preparations from washed blood cells; nitric oxide hemoglobin and sulfhemoglobin. *J. Biol. Chem.* 112(1), 51–65 (1935).

20 Sheng K, Pietersz GA, Wright MD, Apostolopoulos V. Dendritic cells: activation and maturation-applications for cancer immunotherapy. *Curr. Med. Chem.* 12(15), 1783–1800 (2005).

21 Prabhu RH, Patravale VB, Joshi MD. Polymeric nanoparticles for targeted treatment in oncology: current insights. *Int. J. Nanomedicine* 10, 1001 (2015).

22 Rosalia RA, Cruz LJ, van Duikeren S *et al.* CD40-targeted dendritic cell delivery of PLGA-nanoparticle vaccines induce potent anti-tumor responses. *Biomaterials* 40, 88–97 (2015).

• **Throws light on the recent advances and ongoing clinical trials on targeted polymeric nanocarriers in the field of oncology.**

23 Joshi VB, Geary SM, Salem AK. Biodegradable particles as vaccine delivery systems: size matters. *AAPS J.* 15(1), 85–94 (2013).

•• **Indicates how size of the particulate vaccine carriers affects the magnitude of Ag-specific immune response.**

24 Zhao L, Seth A, Wibowo N *et al.* Nanoparticle vaccines. *Vaccine* 32(3), 327–337 (2014).

25 Honary S, Zahir F. Effect of zeta potential on the properties of nano-drug delivery systems-a review (Part 2). *Trop. J. Pharmaceut. Res.* 12(2), 265–273 (2013).

26 Thamake SI, Raut SL, Ranjan AP, Gryczynski Z, Vishwanatha JK. Surface functionalization of PLGA nanoparticles by non-covalent insertion of a homo-bifunctional spacer for active targeting in cancer therapy. *Nanotechnology* 22(3), 035101 (2011).

27 Fröhlich E. The role of surface charge in cellular uptake and cytotoxicity of medical nanoparticles. *Int. J. Nanomedicine* 7, 5577 (2012).

28 Yue Z, Wei W, Lv P *et al.* Surface charge affects cellular uptake and intracellular trafficking of chitosan-based nanoparticles. *Biomacromolecules* 12(7), 2440–2446 (2011).

29 Ranjan AP, Mukerjee A, Helson L, Vishwanatha JK. Scale up, optimization and stability analysis of Curcumin C3 complex-loaded nanoparticles for cancer therapy. *J. Nanobiotechnol.* 10(38), 20 (2012).

30 Melief CJ. Cancer immunotherapy by dendritic cells. *Immunity* 29(3), 372–383 (2008).

31 Ardavín C, Amigorena S, de Sousa CR. Dendritic cells: immunobiology and cancer immunotherapy. *Immunity* 20(1), 17–23 (2004).

32 Cella M, Sallusto F, Lanzavecchia A. Origin, maturation and antigen presenting function of dendritic cells. *Curr. Opin. Immunol.* 9(1), 10–16 (1997).

33 Ikeda H, Old LJ, Schreiber RD. The roles of IFNγ in protection against tumor development and cancer immunoediting. *Cytokine Growth Factor Rev.* 13(2), 95–109 (2002).

34 Schroder K, Hertzog PJ, Ravasi T, Hume DA. Interferon-gamma: an overview of signals, mechanisms and functions. *J. Leukoc. Biol.* 75(2), 163–189 (2004).

•• **Discusses plausible IFN-γ-dependent antitumor defense mechanisms and indicates IFN-γ as a key player of the immune system regulating tumor development.**

35 Lamagna C, Aurrand-Lions M, Imhof BA. Dual role of macrophages in tumor growth and angiogenesis. *J. Leukoc. Biol.* 80(4), 705–713 (2006).